Absolute Total Electron Impact Ionization Cross-Sections for Many-Atom Organic and Halocarbon Species

ARTICLE *in* THE JOURNAL OF PHYSICAL CHEMISTRY A · DECEMBER 2011

Impact Factor: 2.69 · DOI: 10.1021/jp210294p · Source: PubMed

3 AUTHORS, INCLUDING:

James N. Bull
University of Melbourne
23 PUBLICATIONS **76** CITATIONS
SEE PROFILE

Claire Vallance
University of Oxford
91 PUBLICATIONS **1,135** CITATIONS
SEE PROFILE

THE JOURNAL OF PHYSICAL CHEMISTRY A

ARTICLE

pubs.acs.org/JPCA

Absolute Total Electron Impact Ionization Cross-Sections for Many-Atom Organic and Halocarbon Species

James N. Bull,[†] Peter W. Harland,[‡] and Claire Vallance*[,†]

[†]Chemistry Research Laboratory, Department of Chemistry, University of Oxford, 12 Mansfield Road, Oxford OX1 3TA, United Kingdom

[‡]Department of Chemistry, University of Canterbury, Private Bag 4800, Christchurch 8140, New Zealand

Supporting Information

ABSTRACT: The experimental determination of absolute total electron impact ionization cross-sections for polyatomic molecules has traditionally been a difficult task and restricted to a small range of species. This article reviews the performance of three models to estimate the maximum ionization cross-sections of some 65 polyatomic organic and halocarbon species. Cross-sections for all of the species studied have been measured experimentally using the same instrument, providing a complete data set for comparison with the model predictions. The three models studied are the empirical correlation between maximum ionization cross-section and molecular polarizability, the well-known binary encounter Bethe (BEB) model, and the functional group additivity model. The excellent agreement with experiment found for all three models, provided that calculated electronic structure parameters of suitably high quality are used for the first two, allows the prediction of total electron-impact ionization cross-sections to at least 7% precision for similar molecules that have not been experimentally characterized.

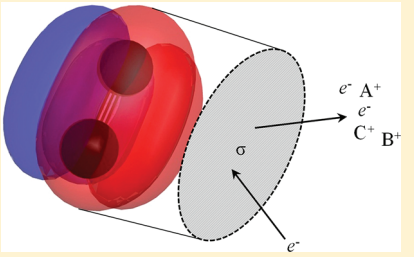

1. INTRODUCTION

Electron collisions with matter leading to ionization represent one of the most fundamental processes in collision physics. In the gas phase, the total efficiency of the process is described by the absolute total electron-impact ionization cross-section, σ. Knowledge of σ is important for a variety of applications, including calibration and normalization of experimental mass spectrometry data, the estimation of other related molecular properties such as polarizabilities, the understanding of biological electron ionization damage, and the modeling of plasmas, gas discharges, and processes in the interstellar medium.[1] Although the application of electron impact ionization in mass spectrometry was suggested nearly 100 years ago,[2] experimentally measured values of σ have only been reported for atoms and a series of small inorganic and organic species. Experimentally, at low electron energies, σ is found to rise from zero above a threshold corresponding to the ionization energy, before reaching a maximum and tapering off at higher energies. This behavior may be understood in terms of a model in which σ reaches a maximum, σ_{max}, when the de Broglie wavelength of the incident electron is in resonance with the highest occupied molecular orbital (HOMO) or is a close match to a typical bond length of 1.3−1.4 Å. For polyatomic organic species this typically occurs in the range of 70−80 eV, close to the standard used in analytical mass spectrometry of 70 eV.

The direct measurement of absolute cross-sections is challenging, and in most cases relative cross-sections are measured instead. A calibration is then required in order to convert the measured relative cross-sections into absolute values, with the consequence that there is considerable variation between reported cross-sections measured using different experimental setups. The largest body of recent absolute measurements recorded on a single instrument is that of Harland and co-workers, which includes a series of saturated halocarbons;[3−5] C_1−C_4 alcohols;[6] C_2−C_6 methanoate and C_3−C_7 ethanoate esters;[7] C_2−C_4 aldehydes, C_3−C_6 ketones, and C_2 and C_4 C_{2V}-symmetric ethers.[8] This set of 65 species will be denoted herein as "the experimental data set". The instrument used for these measurements was a total current counting apparatus and is described in detail in ref 3. The maximum size of molecules studied was limited by the fact that the instrument utilized a room-temperature effusive source, requiring species to be thermally stable and have a reasonable room-temperature vapor pressure.

Theoretically, rigorous quantum mechanical calculation of σ is a many-body problem and is only feasible for atoms and atomic ions. There are several approximate semiempirical and semiclassical models that are mainly restricted to point-like species; these have been reviewed by Deutsch, Becker, Matt, and Märk[9] and by Harland and Vallance.[10] The majority of these models are based on the additivity concept,[11] according to which σ is determined as a sum of contributions from atomic orbitals, molecular orbitals, or even functional groups. Of particular note is the point-like Binary-Encounter-Bethe (BEB) model of Kim and Rudd,[12,13]

Received: October 26, 2011
Revised: December 3, 2011
Published: December 05, 2011

Table 1. Computed $\langle\alpha\rangle_{ele}$ for Small Molecules

	electronic static isotropic polarizability, $\langle\alpha\rangle_{ele}$/Å^3						
level of theory	CO[a]	H_2O	NH_3	CH_4	HF	CF_4	rmsd[b]
CCSD//Sadlej(H+d)	1.93	1.44	2.12	2.50	0.83	2.82	0.03
CCSD//cc-pVTZ	1.67	1.02	1.59	2.18	0.52	2.21	0.45
CCSD//aug-cc-pVTZ	1.92	1.37	2.04	2.41	0.78	2.74	0.09
CCSD//cc-pVQZ	1.79	1.15	1.75	2.29	0.62	2.47	0.30
CCSD(T)//Sadlej(H+d)	1.96	1.47	2.16	2.53	0.85	2.89	0.03
CCSD(T)//aug-cc-pVTZ	1.93	1.41	2.09	2.44	0.80		0.07
PBE0//Sadlej(H+d)	1.93	1.45	2.14	2.56	0.85	2.85	0.02
experimental[c]	1.94	1.45	2.16	2.56	0.82	2.83	

[a] Number of spherical harmonic basis functions are 48, Sadlej(H+d); 60, cc-pVTZ; 92, aug-cc-pVTZ; 110, cc-pVQZ. [b] Root-mean-squared-displacement calculated as rmsd = $\{[\Sigma_{i=1}^{n}((\langle\alpha\rangle_{ele,expt})_i-(\langle\alpha\rangle_{ele,calc})_i))^2]/n\}^{1/2}$, for n = 6 (5 for CCSD(T)//aug-cc-pVTZ). [c] Tabulated in refs 24, 45, and 46.

based on integration of the Binary-Encounter-Dipole (BED) differential cross-section model from the same authors. To date, most of these models have only been applied to atomic and small polyatomic species, and there has been no detailed consideration of molecules with more than a few atoms.

In 1957, Lampe, Franklin, and Field[14] were the first to notice an empirical relationship between mean (isotropic) dipole polarizability volume, $\langle\alpha\rangle$, and σ_{max}, an observation that has been confirmed subsequently by several studies.[8,15−20] The correlation has been rationalized by the fact that, theoretically, both properties have an analogous mathematical dependence on the electronic dipole matrix.[14] The atomic or molecular polarizability is formally represented by a Cartesian symmetric tensor of second rank, $\boldsymbol{\alpha}$, with the mean isotropic polarizability, or "polarizability volume" defined as

$$\langle\alpha\rangle = \frac{1}{3}Tr(\boldsymbol{\alpha}) \quad (1)$$

Assuming the Born−Oppenheimer approximation, $\langle\alpha\rangle$ can be separated into electronic and vibrational terms, denoted $\langle\alpha\rangle_{ele}$ and $\langle\alpha\rangle_{vib}$, respectively. Experimentally determined values of $\langle\alpha\rangle$ have only been reported for a selection of small molecules, and there can be substantial variance between different experimental values for the same molecule.[7] Previous investigations into the relationship between measured values of σ_{max} and values of $\langle\alpha\rangle$ reported in the literature have demonstrated a good correlation between the two properties, though with substantial scatter, which was assumed to arise partly from uncertainties in the published polarizabilities.[8,15]

The work in this article endeavors to review the performance of the empirical polarizability, BEB, and simple functional group additivity models in determining σ_{max} across the entire experimental data set. First, a computational procedure is developed to allow accurate calculation of $\langle\alpha\rangle$, allowing an improved linear correlation with σ_{max} to be found. Next, the BEB model is assessed using the same high-level systematic approach to calculate orbital parameters for all species, therefore, eliminating different computational levels of theory for different species as a source of variation between BEB and experimental σ_{max}. Finally, the reliability of the functional group additivity model is reviewed statistically using a new set of simultaneously refined parameters based on fitting all experimental data.

2. COMPUTATIONAL METHODS

All calculations were performed using the Gaussian 09 and GAMESS-US (October 2010 release) computational packages.[21,22] The CCSD(T) second-order density matrix properties reported in section 3.1 were computed using the CFOUR package.[23]

The accurate calculation of static dipole polarizabilities and hyperpolarizabilities requires a suitably polarized basis set and inclusion of electron correlation. Based on a related study by Sekino and Bartlett[24] and preliminary calculations carried out herein, the Sadlej[25] triple-ζ quality basis, originally developed for polarizability calculations, was adopted. All nonhydrogen atoms utilized the default basis, while the hydrogen basis was augmented with one set of additional uncontracted *d* functions with orbital exponent ζ = 0.1. This modified basis set is denoted as Sadlej(H+d) herein. For each species, geometrical optimizations were performed, followed by polarizability and frequency calculations, to ensure a minimum energy structure. The PBE0 DFT functional was adopted due to excellent performance in other polarizability calculations.[26,27]

For BEB calculations, vertical ionization potentials were determined using three different methods: SCF-reference Koopman's theorem; OVGF electron propagator theory (EPT);[28] P3 EPT;[29] and EOM-IP-CCSD.[30] In each case, the geometry employed was that optimized at the respective level of theory. The last method was only applied as a benchmark for several small species in order to assess the suitability of EPT methods. The Dunning and co-workers[31,32] aug-cc-pVTZ basis set was adopted for these calculations due to good agreement with experimental vertical ionization potentials (IP_V).

3. RESULTS AND DISCUSSION

3.1. Static Polarizability Correlation. To calculate accurate polarizabilities for all species in the experimental data set, the first requirement was the determination of a suitable level of theory. Initially, following Sekino and Bartlett,[24] calculations were performed using various levels of theory on several small and well-characterized molecules that represent bond moieties for species in the experimental data set. The results of these calculations are summarized in Table 1. The root-mean-squared deviation, rmsd, for each level of theory indicates the importance of diffuse and diffuse-polarization functions in providing an accurate description of the polarizability. The data indicate that the smaller Sadlej(H+d) basis set, which is optimized for polarizability

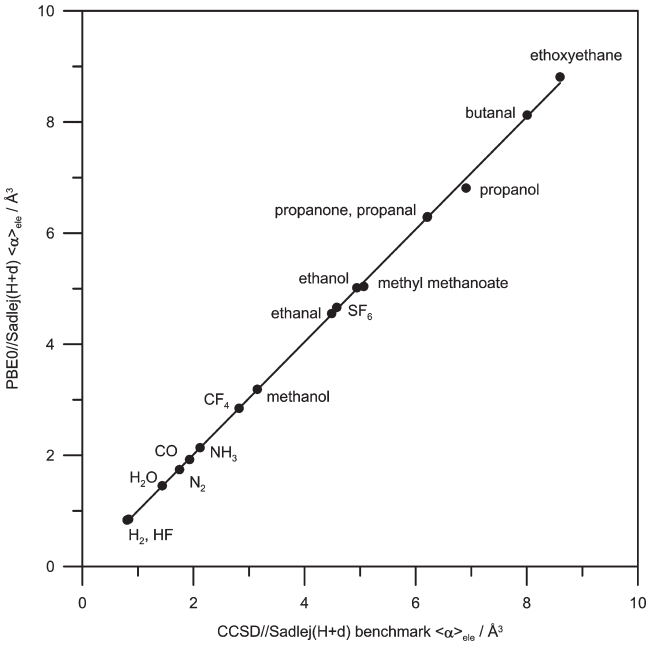

Figure 1. Correlation between PBE0//Sadlej(H+d) and CCSD//Sadlej(H+d) benchmark $\langle\alpha\rangle_{ele}$ for a series of moiety species; R^2 = 0.999 and slope =1.013.

calculations, performs substantially better than larger correlation-consistent basis sets, and also reveal that the PBE0//Sadlej(H+d) method, also specifically designed for polarizability calculations, gives near identical performance to the more expensive CCSD//Sadlej(H+d) or CCSD(T)//Sadlej(H+d) levels of theory. The excellent performance of PBE0//Sadlej(H+d) against a CCSD//Sadlej(H+d) benchmark also extends to considerably larger molecules, as shown in Figure 1. The Dunning and co-workers bases can be improved for polarizability calculations by including an optimized series of additional diffuse functions.[33] However, this routinely becomes prohibitively expensive for molecules containing more than a few atoms. Use of PBE0 rather than CCSD is highly desirable for larger organic species due to the fourth-order scaling of the calculation with molecular size, in contrast to the sixth-order scaling of CCSD. Having identified a level of theory that produces accurate polarizabilities across the range of species considered, the computational method can now be eliminated as a factor in any observed disagreement with empirical trends.

Values of $\langle\alpha\rangle_{ele}$ calculated using PBE0//Sadlej(H+d) for species in the experimental data set are given in Table 2, along with experimentally measured σ_{max}. The empirical correlation of $\langle\alpha\rangle_{ele}$ with σ_{max} is shown in Figure 2 and displays a strong linear dependence of σ_{max} on $\langle\alpha\rangle_{ele}$. The plot in Figure 2 has $R^2 = 0.979$, with a corresponding 95% confidence interval uncertainty of about 7% across 63 organic and halocarbon species in the experimental data set. This represents a considerable improvement over the correlations reported previously with $R^2 = 0.943$ and a 95% confidence interval uncertainty of about 30% for around 30 species, which was based on available $\langle\alpha\rangle_{ele}$ values from the literature.[8] No sufficient statistical evidence was found within this data set to support a different correlation for halocarbon and organic species within the above confidence limits. Two species, CH_3Br and $CF_2CFCFCF_2$, have been omitted from the plot in Figure 2. These two species lie well away from the line of best fit, with either the calculated polarizability being too large or the

Table 2. Cross-Section[a] and Polarizability Parameters for All Species

species	σ_{max}/Å^2	σ_{BEB}/Å^2	$\langle\alpha\rangle_{ele}$/Å^3
Alcohols[b]			
methanol	4.61(18)	5.11	3.18
ethanol	7.60(30)	8.02	5.00
propanol	10.15(41)	10.94	6.81
propan-2-ol	10.24(41)	10.86	6.82
butanol	12.85(51)	13.91	8.65
butan-2-ol	13.06(52)	13.91	8.62
2-methylpropan-1-ol	13.33(53)	14.25	8.54
2-methylpropan-2-ol	13.41(54)	13.53	8.57
Aldehydes[c]			
ethanal	6.7(3)	6.86	4.55
propanal	9.7(4)	9.79	6.28
butanal	12.4(5)	12.55	8.11
2-methyl-propanal	11.9(5)	12.41	8.11
Ethers[c]			
ethoxyethane	14.2(6)	14.20	8.81
propoxypropane	17.8(7)	19.65	12.28
2-methylethoxy-2-methylethane	19.6(8)	20.03	12.15
Esters[d]			
methyl methanoate	7.6(3)	8.28	5.07
ethyl methanoate	10.4(4)	10.40	6.93
propyl methanoate	13.6(5)	14.23	8.77
2-methylethyl methanoate	13.0(5)	13.67	8.67
butyl methanoate	15.6(6)	16.95	10.64
3-methylpropyl methanoate	15.6(6)	17.05	10.50
pentyl methanoate	18.8(8)	19.90	12.52
methyl ethanoate	10.5(4)	11.02	6.87
ethyl ethanoate	13.8(6)	13.91	8.74
propyl ethanoate	15.7(6)	16.86	10.59
2-methylethyl ethanoate	15.2(6)	17.03	10.49
butyl ethanoate	18.3(7)	19.81	12.47
3-methylpropyl ethanoate	18.3(7)	20.03	12.29
2-methylpropyl ethanoate	18.2(7)	20.02	12.29
2,2-dimethylethyl ethanoate	18.5(7)	20.04	12.20
Ketones[c]			
propanone	9.0(4)	9.79	6.30
butanone	12.3(5)	12.50	8.05
pentan-2-one	14.9(6)	15.74	9.90
pentan-3-one	15.4(6)	15.85	9.80
3-methylbutan-2-one	15.1(6)	15.49	9.79
hexan-2-one	17.1(7)	18.74	11.76
hexan-3-one	16.9(7)	18.86	11.67
3,3-dimethylbutan-2-one	16.9(7)	18.47	11.51
3-methylpentan-2-one	17.0(7)	18.67	11.56
4-methylpentan-2-one	17.1(7)	18.72	11.66
Halocarbons[e,f]			
CH_3F	3.72(15)	4.39	2.56
CF_3H	4.32(17)	6.12	2.77
CF_4	4.75(19)	5.84	2.85
C_2F_4	5.90(24)	8.77	4.35

dx.doi.org/10.1021/jp210294p |J. Phys. Chem. A 2012, 116, 767–777

Table 2. Continued

species	σ_{max}/Å^2	σ_{BEB}/Å^2	$\langle\alpha\rangle_{ele}$/Å^3
C_2F_6	7.64(31)	10.08	4.78
C_3F_8	10.33(41)	14.22	6.70
CF_2CFCF_3	8.83(35)	12.91	6.41
CF_3CCCF_3	10.27(41)	15.50	7.94
$CF_2CFCFCF_2$	10.46(42)	14.95	8.75
$CF_3CFCFCF_3$	11.60(46)	15.51	8.48
CF_3CN	6.33(25)	9.53	4.72
CH_3Cl	6.91(28)		4.42
$CHCl_3$	12.25(49)		8.49
CF_3Cl	6.93(28)		4.69
CF_2Cl_2	9.57(38)		6.61
CCl_3CN	14.11(56)		10.56
CH_3Br	8.02(3)		5.47
$CHBr_3$	13.75(55)		11.72
CH_2Br_2	11.67(47)		8.60
CBr_4	19.0(8)		14.73
CH_3I	10.3(4)		7.38
Others[b–f]			
N_2	2.53(10)		2.14
CH_4	4.24(17)		2.56
SF_6	7.10(28)		4.66
CH_3CN	6.33(25)	6.55	4.43
Amides[g]			
methyl ethanamide	11.44	11.98	7.70
ethyl ethanamide	14.10	14.89	9.49
dimethyl methanamide	14.16	14.94	9.53

[a] Maximum instrumental errors given in parentheses. [b] Ref 6. [c] Ref 8. [d] Ref 7. [e] Ref 3. [f] Ref 5. [g] Calculated from eq 2.

measured σ_{max} too small. Based on the observed linear correlation of σ_{max} for CH_4, CH_3Br, CH_2Br_2, and CBr_4 with the number of bromine atoms (with R^2 = 1.00), the reported measurement for $CHBr_3$ is thought to be erroneously small, at 13.8(6) Å^2, and would be predicted to be 15.3 Å^2 based on this trend. The situation is similar for $CF_2CFCFCF_2$. Ideally, these two species should be experimentally redetermined.

If instead of considering the correlation of σ_{max} purely with the electronic polarizability $\langle\alpha\rangle_{ele}$, vibrational corrections were included, the correlation was found to be slightly worse for the larger molecular species. This is probably explained by the fact that the calculation of accurate $\langle\alpha\rangle_{vib}$ parameters for large molecules with several conformations is difficult due to the number of low-energy conformations that exist at room temperature. Different conformations tend to have different vibrational contributions to the polarizability, though the electronic contributions are virtually identical. Another correlation that has been suggested based on semiclassical arguments is that between σ_{max} and $(\langle\alpha\rangle_{ele}/IP_V)^{1/2}$, where IP_V is the molecular vertical ionization potential.[15] Application of this correlation using P3 electron propagator IP_V data (section 3.2) indicated no statistical improvement. While this second relation has been shown to fit better to atomic σ_{max} data, the first ionization potential is relatively constant across the organic functional groups in the series considered here, such that differences in $\langle\alpha\rangle_{ele}$ dominate the σ_{max} dependence.

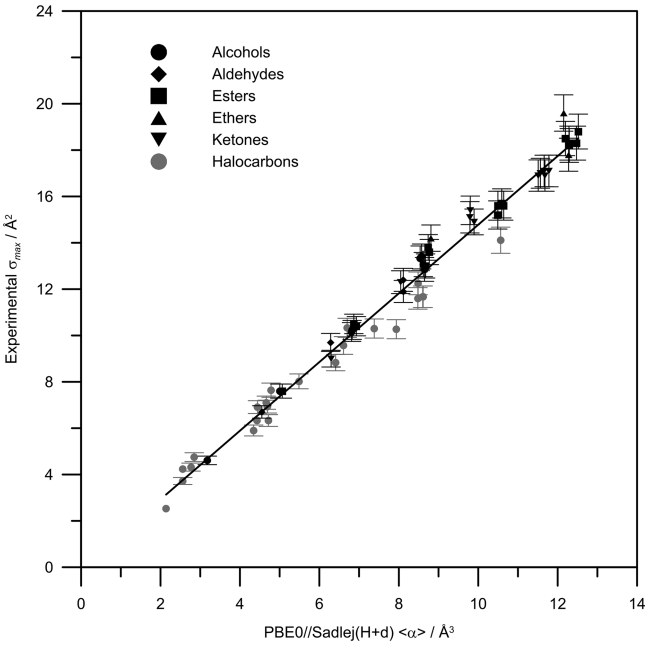

Figure 2. Empirical correlation between experimental σ_{max} and PBE0//Sadlej(H+d) $\langle\alpha\rangle_{ele}$for 63 medium size organic and halocarbon species; R^2 = 0.979 and slope = 1.478.

The observed correlation between $\langle\alpha\rangle$ and σ has traditionally been used to approximate $\langle\alpha\rangle$ from the results of σ measurements. With the demonstrated ease of calculation of $\langle\alpha\rangle_{ele}$ using ab initio or DFT methods, the contrary is now true; σ_{max} can be approximated for species similar to those in the experimental data set based on the calculated polarizabilities. From the fit to the plot in Figure 2, the two parameters are related by the empirical expression

$$\sigma_{max} = (1.478)\langle\alpha\rangle_{ele} \quad (2)$$

where σ_{max} has units of Å^2, $\langle\alpha\rangle_{ele}$ of Å^3, and the proportionality constant of Å^{-1}.

One series of species for which an accurate knowledge of σ would be of considerable interest are the saturated amides, which represent prototypes for studies of the peptide bond. Due to the strong intermolecular hydrogen bonding in these species, the smaller amide species all have high melting points and low vapor pressures and have not been characterized using the room temperature effusive gas source used to study the 65 species reviewed here. Predicted σ_{max} values for the three most common prototypes, calculated using the approach described above, are given in Table 2.

3.2. BEB Cross-Sections. The BEB model developed by Kim and Rudd[12,13] for calculation of total electron impact ionization cross-sections is an integrated approximation to the BED differential cross-section model from the same authors. Briefly, the BED model is based on a weighted combination of two different theories: modified Mott theory for "hard" or small-impact parameter collisions and Bethe cross-section theory (first logarithmic term in eq 3) for "soft" or large-impact parameter collisions, which are dominated by the dipole term. The total BEB cross-section, σ_{BEB}, is given by

$$\sigma_{BEB} = \sum_{orbitals} \left\{ \left(\frac{S}{t + (u+1)} \right) \left[\frac{Q \ln t}{2} \left(1 - \frac{1}{t^2} \right) + (2 - Q) \left(1 - \frac{1}{t} - \frac{\ln t}{t+1} \right) \right] \right\} \quad (3)$$

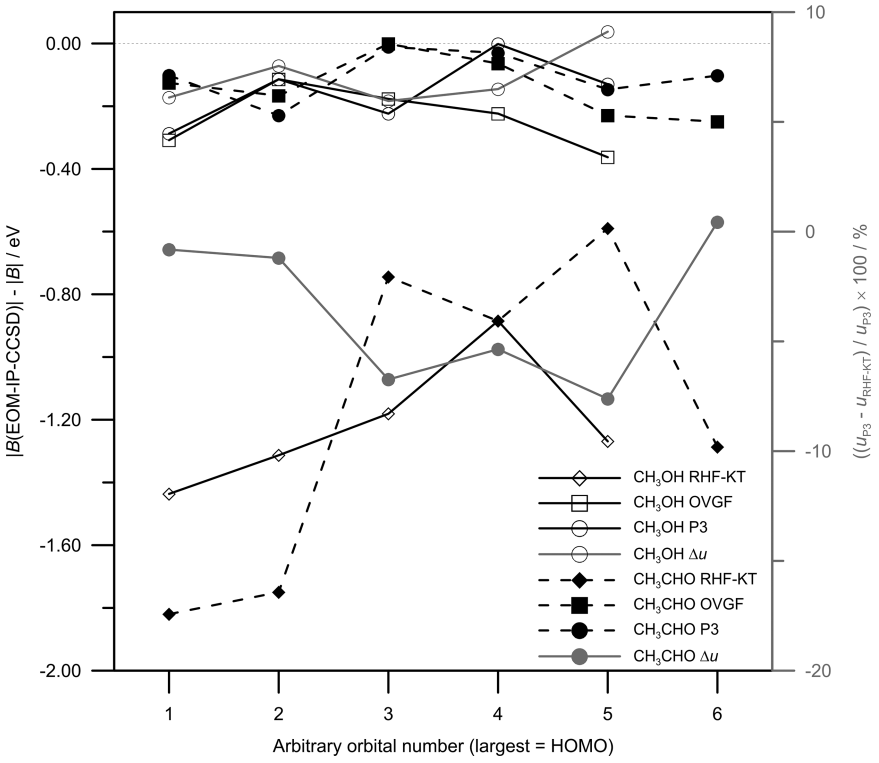

Figure 3. Performance of SCF-reference Koopmans' theorem (RHF-KT), OVGF, and P3 electron propagator methods against an EOM-IP-CCSD benchmark for calculations on methanol and ethanal. Figure is outlined in detail in the text.

where

$$t = \frac{T}{B} \quad u = \frac{U}{B} \quad S = 4\pi a_0^2 N \left(\frac{R}{B}\right)^2$$

In these expressions, T is the kinetic energy of the incident electron and B and U are the orbital binding and kinetic energies, respectively, of the ejected electron. N is the orbital occupancy, a_0 is the Bohr radius, and R is the Rydberg constant. Q represents a dipole oscillator parameter for a given molecule and is defined in terms of ionization to a continuum state. This parameter has not been measured for most molecules. However, a series of publications by the authors of the BEB model have found the approximation of $Q = 1$ to reproduce σ satisfactorily across a variety of molecules from H_2 to SF_6, and the same approximation is therefore made in the present work.[13,34,35] Within the framework of the Bethe−Born theory, this approximation is quite reasonable; in O_2, for example ($IP_V \sim 12.3$ eV), the normalized photoionization cross-section efficiency quantity comparable with Q is relatively energy independent, with a value close to unity over the measured range of 20−75 eV.[36]

The BEB model is most sensitive to the parameter u, the ratio of orbital kinetic and binding energies, for the most weakly bound orbitals. Several different electronic structure schemes have routinely been used to obtain B and U parameters for small molecules combined with experimental values when available. The authors of the BEB theory have noted that the use of experimental rather than calculated values for IP_V ensures a correct threshold and gives slightly better agreement with experiment for the σ of small molecules. This is not surprising considering that the HOMO plays the dominant role in the electron impact process, making a contribution of around 80% to maximum σ_{BEB}.[13,34] Reliable vertical ionization data is not available for the majority of the organic species considered in this work, although all exhibit a similar HOMO IP_V in the range from 10−11 eV. Many reported BEB calculations have utilized SCF-reference or a partially correlated Koopmans' theorem interpretation to obtain all other required binding energies. However, this method is not usually reliable as it lacks any inclusion of electron correlation or orbital relaxation effects accompanying ionization, which can be substantial.[37] Moreover, the larger chain length of the molecules studied in this work means that there are many relatively weakly bound orbitals that all additively contribute significantly to σ. Calculations herein of B and U for each molecule in the experimental data set involved optimization with the aug-cc-pVTZ basis followed by binding energy calculations using the OVGF and P3 electron propagator theory (EPT) methods.

To demonstrate the good performance of the EPT method, several vertical benchmark calculations were performed at the highly correlated EOM-IP-CCSD//aug-cc-pVTZ level of theory, although the sixth-order computational scaling restricts application to molecules with only a few heavy atoms. Comparison of the performance of each method is given in Figure 3 for methanol and ethanal. Figure 3 shows the performance of these different approximations for the five outermost filled orbitals for methanol and six outermost for ethanal. The parameter plotted in black on the left-hand axis is the difference between the result of each method and the EOM-IP-CCSD benchmark calculations; that is, $|B(\text{EOM-IP-CCSD})| - |B(\text{P3})|$. Also plotted in gray on the right-hand axis in Figure 3 is the difference between the Koopmans' theorem determination of BEB parameter u and the P3-determined value. The EOM-IP-CCSD//aug-cc-pVTZ method predicts vertical ionization potentials of 10.98 and 10.25 eV for methanol and ethanal, respectively, which can be compared very

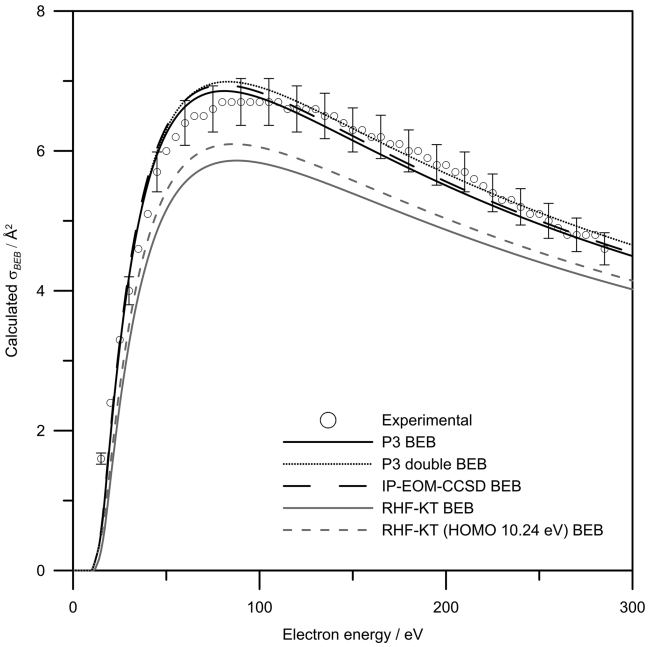

Figure 4. BEB total ionization cross-section calculated using different orbital binding and kinetic energy parameters. SCF-reference Koopmans' theorem RHF-KT (HOMO 10.24 eV) BEB has the HOMO *B* parameter taken as the experimental IP_V. P3 double BEB considers double ionization for inner-shell orbitals (see the discussion in the text).

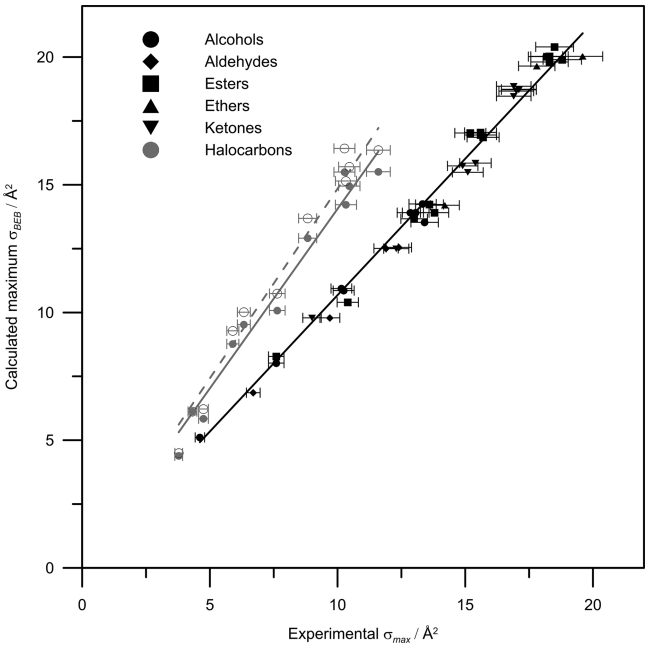

Figure 5. Correlation between calculated maximum σ_{BEB} and experimental σ_{max} for all organic and fluorocarbon species studied. Open circles and the dashed best fit correspond to approximated correction for double ionization processes (see the discussion in the text).

favorably with values of 10.96 and 10.24 eV determined experimentally by photoelectron spectroscopy.[38] Overall, it is observed that the P3 EPT method performs slightly better than OVGF, and this first method was adopted for all remaining species. Figure 3 shows that the SCF-reference Koopmans' theorem calculations predict *B* parameters that are, on average, overestimated by around 1 eV. For CH_3OH this corresponds to an average difference in parameter *u* of ~+7%, while for CH_3CHO the average difference is ~−5%, in comparison with P3 parameters. It has been well-documented previously that Koopmans' theorem overestimates orbital binding energies by around 15%, with the consequence that BEB calculations employing these binding energies systematically underestimate σ.[34,39] The objective of this exercise was to provide a set of very accurate orbital parameters for each molecule under study so that the intrinsic performance of the BEB model could be assessed fairly, without its performance being degraded by the use of ab initio input data of insufficiently high quality. Differences between orbital binding parameters for some larger molecules with several low energy conformations relative to the minimum energy conformation were determined to be negligibly small.

It is of interest to consider the variation in maximum σ_{BEB} when orbital parameters obtained from different orbital binding approximations are employed in the calculations. For methanol, with an experimentally determined σ_{max} of 4.6(2) Å^2; the use of SCF-reference Koopmans' theorem data yielded a maximum σ_{BEB} of 4.54 Å^2, P3 EPT data yielded 5.11 Å^2 and full IP-EOM-CCSD data yielded 5.25 Å^2. The corresponding values for ethanal, with an experimentally measured σ_{max} of 6.7(3) Å^2, were 5.86, 6.86, and 6.94 Å^2, respectively. For the latter method, if SCF-reference orbital kinetic energies were used instead of correlated values extrapolated to satisfy the virial ratio, slightly smaller maximum σ_{BEB} values of 5.20 Å^2 for methanol and 6.72 Å^2 for ethanal were obtained. Fortuitously, in this case, the first and least accurate SCF-reference Koopmans' theorem calculation is closest to experiment for methanol. However, the routine application of poor orbital parameters to give fortuitous agreement for an unknown species should never be considered. The BEB ionization efficiency curves for ethanal calculated using each set of orbital parameters are shown in Figure 4.

To facilitate computations on larger molecules, EPT energies were obtained for all orbitals with binding energies $\lesssim$20 eV. For orbitals with binding energies $\gtrsim$20 eV a linear extrapolation of P3 vs SCF-reference Koopmans data provided a correction factor for IPs $\gtrsim$20 eV, and also allowed normalization of computed kinetic energies to satisfy the virial ratio. Incorporation of these tightly bound orbitals contributed typically only a few percent to σ near the maximum in σ_{BEB}. Overall, this procedure provided a set of quite accurate orbital parameters, facilitating a good assessment of the BEB theory across a large range of organic species. Any differences between the experimental and BEB cross-sections can therefore be attributed to the physics of the BEB theory and other processes rather than to the orbital parameters employed. BEB calculations on species containing chlorine, bromine, or iodine atoms have not been considered here due to the previously established need for further empirical corrections.[40] The correlation between the calculated σ_{BEB} and experimental σ_{max} values are shown in Figure 5. The data clearly separate into two different cases: nonfluorinated organic species lie on one line with a slope of 1.068 and R^2 = 0.986; while fluorocarbons lie on a second line with a slope of 1.406 and R^2 = 0.972. In other words, calculated maximum σ_{BEB} for the nonfluorinated species are very consistently, on average, ~7% larger than experiment, while the fluorocarbons are, on average, ~ 40% larger than experiment. Thus, unlike for the polarizability trend above, there appears not to be a single universal relation. The first and obvious reasoning is that all nonfluorinated species have similar functional groups and

electronic structure, which is quite different to the fluorocarbons. The electronegativity of fluorine means that the accurate calculation of orbital binding parameters requires a good polarized triple-ζ basis set combined with high degree of electron correlation. Calculations to assess the influence of basis set (Pople) on fluorocarbon Koopmans' theorem orbital parameters (neglecting orbital relaxation) have been attempted previously;[39] although probably did not incorporate sufficient basis set polarization. Here, for CH_3F, EOM-IP-CCSD//aug-cc-pVTZ yields IP_V values of 13.28 eV and P3 at 13.39 eV, compared to an experimental value of 13.04 eV. Further halocarbon substitution results in slightly worse agreement between theory and experiment. While the P3 parameters for the larger and more highly substituted halocarbons are not as good as those for the organic species, they are still in reasonable agreement with EOM-IP-CCSD and are considerably better than anything obtained from SCF-reference Koopmans' theorem parameters. For comparison, the maximum in σ_{BEB} for CH_3F calculated using the EOM-IP-CCSD binding parameters is 4.33 Å^2 (4.39 Å^2 when the HOMO B is replaced with experimental IP_V), to be compared with 4.39 Å^2 when P3 EPT parameters are employed, and an experimentally measured value of 3.72(15) Å^2.

That the maximum in σ_{BEB} is always larger than the experimentally measured value σ_{max} should not surprise. Theoretically, σ_{BEB} should be considered as an upper-bound, since the model assumes all energy transfer in excess of the ionization threshold results in ionization. In reality, the electron-impact (single) ionization process is competitive with neutral dissociation and multiple ionizations. The latter process is especially true for chlorine-containing or heavier halocarbon species, in which the large number of inner electrons can give rise to electron knock-off cascades at high incident electron impact energies. For molecules containing lighter atoms, Auger mechanisms can occur, in which an inner electron hole is filled by a relaxing outer valence electron and the excess energy is dissipated by ejection of another spatially and energetically local electron. Doubly charged ions are usually unstable and may dissociate into two charged fragments. In the Harland instrument, both doubly charged ions and their fragmentation would contribute to the measured current and therefore total measured σ. An ad hoc correction to the BEB model to account for multiple ionizations has been to double the inner-shell contribution (i.e., the contribution for orbitals with binding energies B greater than ∼30 eV).[35] This results in an ∼5% increase in σ at the high-energy end of the ionization efficiency curve, bringing the model into better agreement with experiment. If this approach is implemented for the fluorocarbons, the result is the points represented by open circles in Figure 5. These yield a best-fit slope of 1.488 and $R^2 = 0.972$, and correspond to a further ∼8% increase in the maximum σ_{BEB}. For CF_4, detailed comparison of the experimental σ with BEB theory and other neutral dissociation cross-section data has revealed that accounting for the branching ratio into the neutral dissociation pathway can bring experiment and theory into very good accord.[35] This is the probable explanation for the different, but species-consistent, trend for the fluorocarbons in Figure 5. The consistency across the fluorocarbons of a maximum in σ_{BEB} that is ∼40% larger than seen in experiments is not too surprising considering the similarity of electronic structure for each fluorocarbon. It should be noted that a modification of the BED model called siBED has been applied to the CF_x and NF_x ($x = 1-3$) species, with the authors claiming that good agreement was found with experiment when allowing for contributions for ion-pair dissociation channels at low energies.[41−43] Unfortunately, application of the siBED model, with an improved description of shielding effects in the long-range dipole potential, is more complicated than the parent BED model. Clearly, experiments to characterize both ionic and neutral products for the fluorocarbon species considered here are warranted.

The root-mean-square error (RMSE) in the maximum σ_{BEB} relative to the experimental values is 0.48 Å^2 for the organic species and 0.71 Å^2 for the fluorocarbon species. The corresponding 95% confidence intervals are ∼7 and ∼13%, respectively. For the fluorocarbons, a larger sample size would probably assist in an improvement of this second statistic. For now, the application of P3//aug-cc-pVTZ assuming $Q = 1$ and combined with the scaling factor found from Figure 5 is anticipated to yield a maximum σ_{BEB} within 5−10% of experimental values. In addition, this model has the advantage of approximating the functional form of the incident electron energy dependence. For ethanal, shown in Figure 4, the P3 and EOM-IP-CCSD are within the maximum instrumental experimental error, although the BEB model appears to systematically underestimate the electron energy corresponding to σ_{max} by 5−10 eV. Again, the consideration of double ionization from inner-shell orbitals helps to shift the peak closer to the experimental curve. Overall, it can be concluded that, for the organic species, application of the BEB model with a series of accurate orbital parameters can produce an energy-dependent σ that is on par with those available from experiment. Again, this is a highly desirable conclusion considering the relative ease of application of the BEB model. Finally, calculated maximum σ_{BEB} values for the amide species prototypical of the peptide bond are given in Table 2. When these calculated curves are scaled by the gradient determined in Figure 5, the predicted σ_{max} values for methyl ethanamide, ethyl ethanamide, and dimethyl methanamide are 11.22, 13.94, and 13.99 Å^2, respectively, and are within ∼0.2 Å^2 of those determined from the polarizability correlation. The two primary ethanamides both have calculated σ_{max} values that are ∼1 Å^2 larger than the respective analogous ester species, which is equal to the expected increase in σ_{max} for an additional −H group from the functional group model (section 3.3).

3.3. Functional Group and Bond Additivities. The functional group and bond additivity model relies on determining contributions σ_i to σ_{max} from individual functional groups and bonds, such that summation of the appropriate contributions yields an estimate of σ_{max} for the molecule of interest, that is,

$$\sigma_{max} = \sum_i (n_i \sigma_i) \quad (4)$$

where n_i is the number of each type of fragment i present in the molecule. This method has been shown previously to reproduce experimental σ_{max} values for alcohols and halocarbons with good accuracy.[5,6,44] Moreover, similar bond additivity models have been established to estimate isotropic polarizabilities, and yielded good accord with experiment.[45−47]

The original set of bond and functional group cross-sections, σ_i, were determined by correlating σ_{BEB} as a function of skeletal chain length for a series of straight-chain species with the same functional group. Here, a more comprehensive evaluation of the functional group and bond additivity method is presented, in which a multidimensional matrix least-squares fitting method is used to refine the σ_i for all moieties simultaneously across *all* species studied. Since the matrix evaluation was mathematically overdetermined, each σ_i returned from the fitting procedure is

Table 3. Functional Group and Bond Additivitiy Contributions to σ_{max}

bond/functional group	cross-section additivity component/Å^2	
	series linear extrapolation[a]	simultaneous least-squares
	all species	halocarbon species only
C-H	1.0	1.00(4)
C-F	1.1	1.12(4)
C-Cl	3.8 for C = 1 4.4 for C > 1	3.71(15)[b]
C-Br	4.5	4.60(19)
C-I	7.3	7.29[c]
C-CN	3.0	2.41(9)
C-C	1.0	0.69(3)
C═C	1.5	1.46(6)
	all species	organic species only
-CH_3 (1° methyl)	4.0[d]	3.92(16)
-CH_2- (2° methyl)	2.6	2.64(11)
-CH- (3° methyl)	4.0[d]	1.25(5)[d]
-OH	1.8	1.18(5) RMSE = 0.31[e]
-CHO (aldehyde)	1.1	2.98(12) RMSE = 0.19[e]
-CO- (ketone)	2.6	1.56(6) RMSE = 0.40[e]
-OCO- (ester)	5.3	2.96(11) RMSE = 0.28[e]
-CH_2-O-CH_2- (α-1° ether)	N/A	5.52(22) RMSE = 0.40[e]
-CH-O-CH- (α-2° ether)	N/A	3.91[c]

[a] Refs 6 and 8. [b] No strong evidence was found for differing C-Cl bond treatments. [c] Functional group contribution based on a single species and, therefore, should be considered as tentative. [d] Determined as combination of C-C and C-H contributions from top section of this table. For —CH- the simultaneous least-squares set of parameters considers only the C-H contribution. [e] RMSE can be considered as the average error for each functional group series. The overall RMSE, for the halocarbons was 0.39 Å^2, and for all 65 species, was 0.37 Å^2.

averaged across the entire data set. Again, $CHBr_3$ was omitted as it appeared to be an outlier in this model.

Intuitively, due to differences in electronic structure and to encompass bonding effects to the largest degree possible, the most accurate additivity determinations are obtained when the extent of bond fragmentation is minimized, i.e. the summation is made over the largest appropriate functional groups for which data are available (and therefore over the fewest possible fragments).[45] The results of the simultaneous least-squares fitting are summarized in Table 3. The simultaneous refinement of halocarbon and organic species σ_i was in fact carried out separately; the C—H group was the only off-diagonal matrix element to link these two data sets and was not treated individually for the organic series for the reasons just outlined, namely that the halocarbon C—H bond is electronically distinct from a C—H bond in a nonhalogenated molecule. As an example of the performance of the model, 2-methylpropyl ethanoate has an experimentally determined σ_{max} of 18.2(7) Å^2, and application of the model employing the parameters from Table 3 yields 3 × -CH_3 + 1 × -CH_2- + 1 × —CH- + 1 × -OCO- = 18.6(7) Å^2. Using the previously published parameters determined from the series of linear compounds, the value of 24.1 Å^2 is obtained. The excellent performance of the simultaneously refined parameters across the experimental data set is demonstrated in Figure 6. While the model requires a considerable amount of experimental data as input in order to determine the various functional group contributions, once this data is available, σ_{max} for similar unknown species can be predicted in a matter of seconds.

As given in Table 3, the RMSE was 0.37 Å^2, indicating that the functional group additivity model yields ∼3% error, approximately equal to the ∼4% maximum instrumental uncertainty for any individual measurement. This excellent agreement obtained from fitting the experimental data set indicates a high degree of consistency between measurements and that the average instrumental error is probably less than the maximum determined value of ∼4%.

It was found that to achieve good model predictions of σ_{max} for all three of the C_{2v} symmetric ethers included in the experimental data set, the functional group contributions from primary and secondary α-carbon ethers needed to be separated. This is probably due to a combination of the electronic effects and the large bond fluxionality introduced by this species. Insufficient ether data is available to develop a rigid functional group contribution for any given ether.

3.4. Application to Other Species. Other than the measurements reviewed here, the most extensive collection of electron impact ionization cross-sections measured on one instrument are those reported by Harrison et al.[17] and by Beran and Kevin,[16] over 40 years ago for some 38 organic and 62 halocarbon species, respectively. Unfortunately, these measurements were performed at the single electron kinetic energy of 75 eV, denoted σ_{75}, for the first study, and 70 eV, denoted σ_{70}, for the second study. Since the electron energy at which ionization is most efficient varies from molecule to molecule, their measured cross-sections do not necessarily correspond to σ_{max}. This is especially true for the halocarbon species, for which the peak in the ionization cross-section typically occurs at energies between 80 and 130 eV,

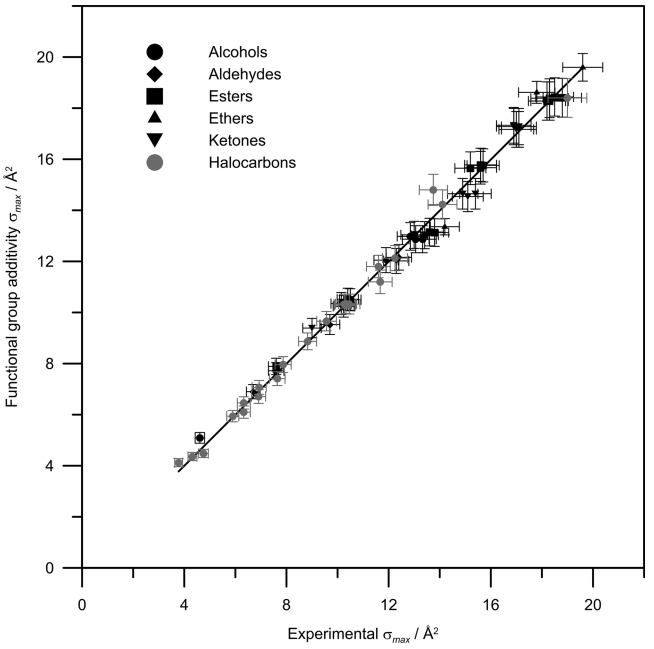

Figure 6. Correlation between the functional group additivity method and experimental data set; $R^2 = 0.992$, slope = 0.999. Vertical error bars are taken from matrix fitted errors.

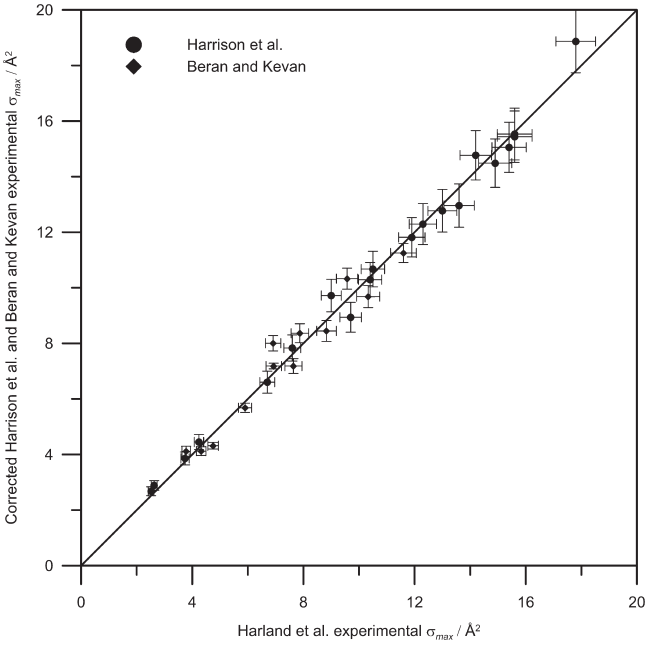

Figure 7. Agreement between the experimental data set and corrected literature data sets (31 species in common). The RMSE is 0.43 Å^3.

significantly higher than the 70 eV used by Beran and Kevin.[16] However, because these data sets have 31 species in common with the Harland et al. experimental data set, correlation between data sets at the same energy is possible. Comparison of the two data sets indicates good monotonic agreement with $R^2 = 0.987$ for a plot of one set of σ_{70} values against the other, but shows the earlier set of cross-sections to be, on average, ~10% larger than those in the more recent experimental data set. This factor may readily be explained following consideration of the calibration

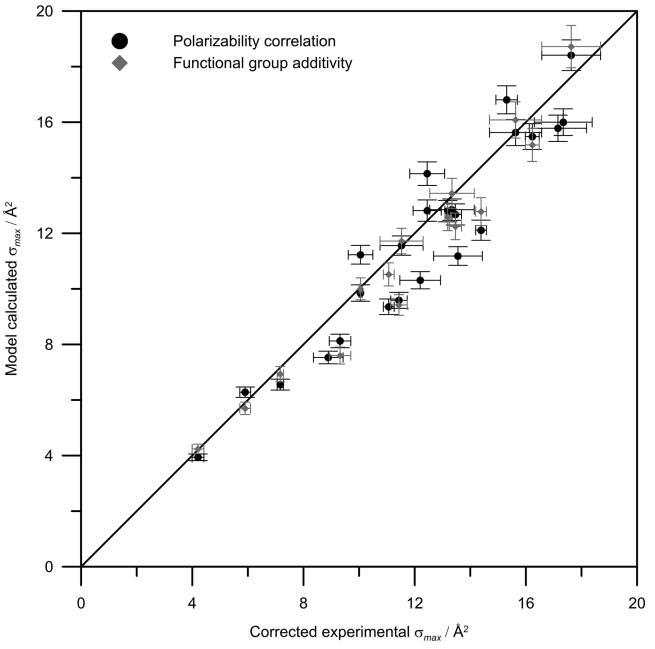

Figure 8. Application of the polarizability correlation and functional group additivity model to corrected experimental cross-sections taken from refs 16 and 17.

procedure employed in the two sets of measurements. Both of the Harrison et al.[17] and Beran and Kevan[16] studies measured relative cross-sections, and converted the results to absolute cross-sections using absolute values for Kr and Ar, respectively, that have now been shown to be incorrect. The authors also reported measurements on the now well-characterized CO, CO_2 and CH_4 species, which were, again, on average, ~10% larger than those measured using the Harland instrument.[48] To compare these earlier data sets with the present experimental data set and with model calculations, the earlier data has been scaled by the correction factor of 0.905, determined by accounting for the calibration errors discussed above. In addition, a second correction factor was determined for each molecule to account for the difference between the literature σ_{75}/σ_{70} and experimental data set σ_{max}. For the Harrison et al.[17] organic species, this second factor was essentially constant at 1.053. The final correlation between these data sets is given in Figure 7, and indicates a high degree of measurement precision between the data sets.

It is an interesting exercise to apply both the polarizability correlation and functional group model to the oxygen-containing organic and halocarbon species measured by Harrison et al.[17] and Beran and Kevan[16] that are not in common with the Harland and co-workers experimental data set. The predictions of both models are plotted against the corrected experimental σ_{max} in Figure 8. It is noted that since a reliable energy-dependent σ measurement was not available for any of these molecules, it was not possible to correct the cross-sections to account for the electron energy at which the measurements were made, rather, an average correction factor value was used. Correspondingly, the agreement of the models with experiment is poorer than that observed for the Harland and co-workers experimental data set. This is almost certainly due primarily to the fact that the majority of molecules in the data set are halocarbon species with σ_{max} occurring at energies 40−70 eV higher than the 70 eV employed for these earlier measurements. The three esters and four nonsymmetric ethers in

dx.doi.org/10.1021/jp210294p |J. Phys. Chem. A 2012, 116, 767–777

Figure 8 are likely to have ionization maxima closest to 75 eV, and are also the species for which agreement with the predictions of the models is most satisfactory. These data do support the assertion that the polarizability correlation and functional group model can give good estimates of σ_{max} for species similar to the experimental data set.

4. CONCLUSIONS

Through statistical analysis of a data set containing 65 different molecules, it has been demonstrated that three simple models for approximating maximum electron impact ionization cross-sections perform very satisfactorily. These models were the empirical polarizability correlation, the binary encounter Bethe model, and the functional group additivity approximation. For all models the errors derived from comparison with experimental data are similar in magnitude to the instrumental errors associated with the experimental measurements. This result supports the contention that these models can determine maximum cross-sections to a *precision* on par with experiment, and application of the correlation factors found herein allow also *accuracy* on par with experiment. Finally, the fact that the models perform very consistently when tested against two experimental data sets recorded using different instruments indicates a high degree of experimental consistency between measurements for each species.

■ ASSOCIATED CONTENT

Supporting Information. Outputs of BEB calculations. This material is available free of charge via the Internet at http://pubs.acs.org.

■ AUTHOR INFORMATION

Corresponding Author
*E-mail: claire.vallance@chem.ox.ac.uk.

■ ACKNOWLEDGMENT

C.V. acknowledges funding from the ERC through Starting Independent Researcher Grant 200733 "ImageMS", from the EPSRC Programme Grant EP/G00224X/1, and from the Marie Curie Initial Training Network 238671 "ICONIC", which has also provided a Marie Curie Postdoctoral Fellowship for J.N.B.

■ REFERENCES

(1) Field, F. H.; Franklin, J. L. *Electron Impact Phenomena and the Properties of Gaseous Ions*; Academic Press, Inc.: New York, 1957.
(2) Thomson, J. J. *Philos. Mag.* **1912**, *23*, 449–457.
(3) Vallance, C.; Harris, S. A.; Hudson, J. E.; Harland, P. W. *J. Phys. B: At., Mol. Opt. Phys.* **1997**, *30*, 2465–2475.
(4) Hudson, J. E.; Vallance, C.; Bart, M.; Harland, P. W. *J. Phys. B: At., Mol. Opt. Phys.* **2001**, *34*, 3025–3039.
(5) Bart, M.; Harland, P. W.; Hudson, J. E.; Vallance, C. *Phys. Chem. Chem. Phys.* **2001**, *3*, 800–806.
(6) Hudson, J. E.; Hamilton, M. L.; Vallance, C.; Harland, P. W. *Phys. Chem. Chem. Phys.* **2003**, *5*, 3162–3168.
(7) Hudson, J. E.; Weng, Z. F.; Vallance, C.; Harland, P. W. *Int. J. Mass Spectrom.* **2006**, *248*, 42–46.
(8) Bull, J. N.; Harland, P. W. *Int. J. Mass Spectrom.* **2008**, *273*, 53–57.
(9) Deutsch, H.; Becker, K.; Matt, S.; Märk, T. D. *Int. J. Mass Spectrom.* **2000**, *197*, 37–69.
(10) Harland, P. W.; Vallance, C. *Adv. Gas Phase Ion. Chem.* **1998**, *3*, 319–358.
(11) Otvos, J. W.; Stevenson, D. P. *J. Am. Chem. Soc.* **1956**, *78*, 546–551.
(12) Kim, Y.-K.; Rudd, M. E. *Phys. Rev. A* **1994**, *50*, 3954–3967.
(13) Hwang, W.; Kim, Y.-K.; Rudd, M. E. *J. Chem. Phys.* **1996**, *104*, 2956–2966.
(14) Lampe, F. W.; Franklin, J. L.; Field, F. H. *J. Am. Chem. Soc.* **1957**, *79*, 6129–6132.
(15) Harland, P. W.; Vallance, C. *Int. J. Mass Spectrom. Ion Proc.* **1997**, *171*, 173–181.
(16) Beran, J. A.; Kevan, L. *J. Phys. Chem.* **1969**, *73*, 3866–3876.
(17) Harrison, A. G.; Jones, E. G.; Gupta, S. K.; Nagy, G. P. *Can. J. Chem.* **1966**, *44*, 1967–1973.
(18) Bartmess, J. E.; Georgiadis, R. M. *Vacuum* **1983**, *33*, 149–153.
(19) Nishimura, H.; Tawara, H. *J. Phys. B: At., Mol. Opt. Phys.* **1994**, *27*, 2063–2074.
(20) Karwasz, G. P.; Brusa, R. S.; Piazza, A.; Zecca, A. *Phys. Rev. A* **1999**, *59*, 1341–1347.
(21) Frisch, M. J.; Trucks, G. W.; Schlegel, H. B.; Scuseria, G. E.; Robb, M. A.; Cheeseman, J. R.; Scalmani, G.; Barone, V.; Mennucci, B.; Petersson, G. A.; et al. *Gaussian 09*, Revision A.1; Gaussian, Inc.: Wallingford, CT, 2009.
(22) Schmidt, M. W.; Baldridge, K. K.; Boatz, J. A.; Elbert, S. T.; Gordon, M. S.; Jensen, J. H.; Koseki, S.; Matsunaga, N.; Nguyen, K. A.; Su, S.; Windus, T. L.; Dupuis, M.; Montgomery, J. A. *J. Comput. Chem.* **1993**, *14*, 1347–1363.
(23) CFOUR, Coupled-Cluster techniques for Computational Chemistry, a quantum-chemical program package by Stanton, J. F.; Gauss, J.; Harding, M. E.; Szalay, P. G. with contributions from Auer, A. A.; Bartlett, R. J.; Benedikt, U.; Berger, C.; Bernholdt, D. E.; Bomble, Y. J.; Christiansen, O.; Heckert, M.; Heun, O.; Huber, C.; et al. and the integral packages MOLECULE (Almlöf, J.; Taylor, P. R.), PROPS (Taylor, P. R.), ABACUS (Helgaker, T.; Jensen, H. J. Aa.; Jørgensen, P.; Olsen, J.), and ECP routines by Mitin, A. V.; van Wüllen, C. For the current version, see http://www.cfour.de.
(24) Sekino, H.; Bartlett, R. J. *J. Chem. Phys.* **1993**, *98*, 3022–3037.
(25) Sadlej, A. J. *Collect. Czech. Chem. Commun.* **1988**, *53*, 1995–2016.
(26) Adamo, C.; Cossi, M.; Scalmani, G.; Barone, V. *Chem. Phys. Lett.* **1999**, *307*, 265–271.
(27) Caillie, C. V.; Amos, R. D. *Chem. Phys. Lett.* **2000**, *328*, 446–452.
(28) von Niessen, W.; Schirmer, J.; Cederbaum, L. S. *Comp. Phys. Rep.* **1984**, *1*, 57–125.
(29) Ortiz, J. V. *J. Chem. Phys.* **1996**, *104*, 7599–7605.
(30) Stanton, J. F.; Gauss, J. *J. Chem. Phys.* **1994**, *101*, 8938–8944.
(31) Dunning, T. H., Jr. *J. Chem. Phys.* **1989**, *90*, 1007–1023.
(32) Kendall, R. A.; Dunning, T. H., Jr.; Harrison, R. J. *J. Chem. Phys.* **1992**, *96*, 6796–6806.
(33) Woon, D. E.; Dunning, T. H., Jr. *J. Chem. Phys.* **1994**, *100*, 2975–2988.
(34) Kim, Y.-K.; Hwang, W.; Weinberger, N. M.; Ali, M. A.; Rudd, M. E. *J. Chem. Phys.* **1997**, *106*, 1026–1033.
(35) Nishimura, H.; Huo, W. M.; Ali, M. A.; Kim, Y.-K. *J. Chem. Phys.* **1999**, *110*, 3811–3822.
(36) Brion, C. E.; Tan, K. H.; van der Wiel, M. J.; van der Leeuw, Ph. E. *J. Electron Spectrosc. Relat. Phenom.* **1979**, *17*, 101–119.
(37) Calabro, D. C.; Lichtenberger, D. L. *Inorg. Chem.* **1980**, *19*, 1732–1734.
(38) Linstrom, P. J.; Mallard, W. G. *NIST Chemistry WebBook, NIST Standard Reference Database Number 69*; National Institute of Standards and Technology: Gaithersburg, MD, August 2011; 20899.
(39) Torres, I.; Martínez, R.; Rayo, M. N. S.; Castaño, F. *J. Chem. Phys.* **2001**, *115*, 4041–4050.
(40) Irikura, K. K.; Ali, M. A.; Kim, Y.-K. *Int. J. Mass Spectrom.* **2003**, *222*, 189–200.
(41) Huo, W. M. *Phys. Rev. A* **2001**, *64*, 042719–16.
(42) Huo, W. M.; Tarnovsky, V.; Becker, K. H. *Chem. Phys. Lett.* **2002**, *358*, 328–336.

(43) Christophorou, L. G.; Olthoff, J. K.; Rao, M. V. V. S. *J. Phys. Chem. Ref. Data* **1996**, *25*, 1341–1388.
(44) Fitch, W. L.; Sauter, A. D. *Anal. Chem.* **1983**, *55*, 832–835.
(45) Miller, K. J. *J. Am. Chem. Soc.* **1990**, *112*, 8533–8542.
(46) No, K. T.; Cho, K. H.; Jhon, M. S.; Scheraga, H. A. *J. Am. Chem. Soc.* **1993**, *115*, 2005–2014.
(47) Beran, J. A.; Kevan, L. *J. Phys. Chem.* **1969**, *73*, 3860–3866.
(48) Hudson, J. E.; Vallance, C.; Harland, P. W. *J. Phys. B: At., Mol. Opt. Phys.* **2004**, *37*, 445–455.